Journal of Machine Engineering, Vol. 11, No. 4, 2011

power monitoring, abrasive machining, grinding, taguchi, wheel wear, CBN

Emma BRAZEL[1]
Raymond HANLEY[2]
Garret E. O'DONNELL[1]

THE EFFECTS OF PROCESS PARAMETERS ON SPINDLE POWER CONSUMPTION IN ABRASIVE MACHINING OF CoCr ALLOY

The production environment requires seamless integration, efficiency and robustness of process monitoring solutions. This research investigates data acquisition on the machine tool through the monitoring of NC kernel data. This approach provides many advantages, particularly in an industrial setting where it may be impractical to install additional sensors for process monitoring. The process investigated is abrasive machining of Cobalt Chrome alloy. Cobalt Chrome alloys are extensively used in the biomedical industry as both femoral and tibial components of prosthetic joints. Abrasive machining or grinding is widely employed as the main method for material removal for these components. Understanding the influence of key variables in such a process is necessary before optimization can be achieved. Significant information can be obtained by utilizing power consumption during machining as a process metric. Power consumption of a spindle during an abrasive machining process of Cobalt Chrome alloy is monitored under various conditions through a machine-NC-based application. The effects of changes in feed rate, wheel speed, depth of cut and tool condition are investigated here through Taguchi experimental design. Experimental results are presented with significant machining variables identified.

1. INTRODUCTION

The manufacturing industry of today is even more competitive as a result of the recent global economic downturn. In order to succeed in this demanding environment it is necessary to ensure a manufacturing enterprise's process is as efficient, precise and productive as can be. For industries typified by intensive machining operations, this can be achieved through process monitoring and optimization [1].

The direct approach to process monitoring is a useful tool in the lab, where external sensors are employed to derive useful information in relation to a process such as direct forces, or in the case of tool wear; machine vision. The indirect method of assessing a process through auxiliary quantities such as power is a more appropriate approach in

[1] Department of Mechanical and Manufacturing Engineering, Trinity College Dublin, Ireland
[2] DePuy Ireland, Johnson & Johson, Loughberg, Ringaskiddy, Co Cork, Ireland

industry, where ease of use, space, setup time and maintenance issues are important considerations.

In many cases, as is found in the orthopedic device industry where five-axis machining is commonplace, the potential of the machine tool as a process monitoring device itself remains under-utilized.

The technologies necessary for these intensive machining operations generally include advanced open-architecture NC control, in particular the Siemens 840D sl control. Open architecture in machine controllers provides an opportunity for the digital data acquisition of machine variables via the numerical control without the need for installation of an additional sensor to monitor the process [2]. Brecher and Quintana et al. successfully implemented digital data acquisition for process monitoring utilizing a NC software trace utility for tool wear monitoring and prediction of surface roughness [3-5]. This software allows the tracing of control internal data including machine data, NC orders and digital drive signals. The current research employs this numerical control data acquisition approach in the study of abrasive machining of CoCr alloy.

Cobalt Chrome alloys are extensively used in the biomedical industry as both femoral and tibial components of prosthetic joints. Typically these alloys have high strength, hardness, wear resistance, and biocompatibility [6]. This makes these materials difficult to machine, and as such abrasive machining is the main method used for material removal. Toric shaped grinding wheels are also typically employed in the abrasive machining process of the implants due to their freeform profiles [7].

For orthopedic implants, it is critical to ensure high quality products in terms of accurate form within tight dimensional tolerances with good surface integrity. To maintain these high standards with high productivity in a cost-effective manner, the manufacturing process chain is subject to continuous optimization. Identifying optimal parameters for the process is important, as is dealing with unavoidable issues such as tool wear in an efficient and cost-effective manner. Electroplated CBN wheels are used in this process due to their high hardness/wear resistance, however the associated power, temperatures and forces for machining with these wheels all increase as they wear [8]. Process monitoring with machine NCK power data may be a useful and appropriate solution for an industrial environment for identifying both tool wear and optimal process parameters. Therefore this paper investigates the influence of cutting conditions on power consumption in the abrasive machining of Cobalt Chrome alloy through a machine kernel data acquisition based approach.

2. EXPERIMENTAL SETUP

Workpiece material was initially supplied for the tests in the form of cast bars of CoCrMo F-75 alloy with a bulk hardness of approximately 37HRC. Test parts in the shape of T-bars were then cut and milled from the cast bars with thickness of 8mm, flat surface area of 68mm x 15mm, designed to fit in the machine fixture. All experiments were carried out on a Haas Multigrind CB 5-axis grinding centre with a maximum spindle rotational speed of 8000rpm and power rating of 30kW. Tools were 200mm diameter

electroplated CBN B301 grit grinding wheels with an inner toric radius of 12mm. Straight surface grinding tests were conducted in the up mode. All tests were performed using an oil-based coolant. The machining setup is shown in Fig. 1.

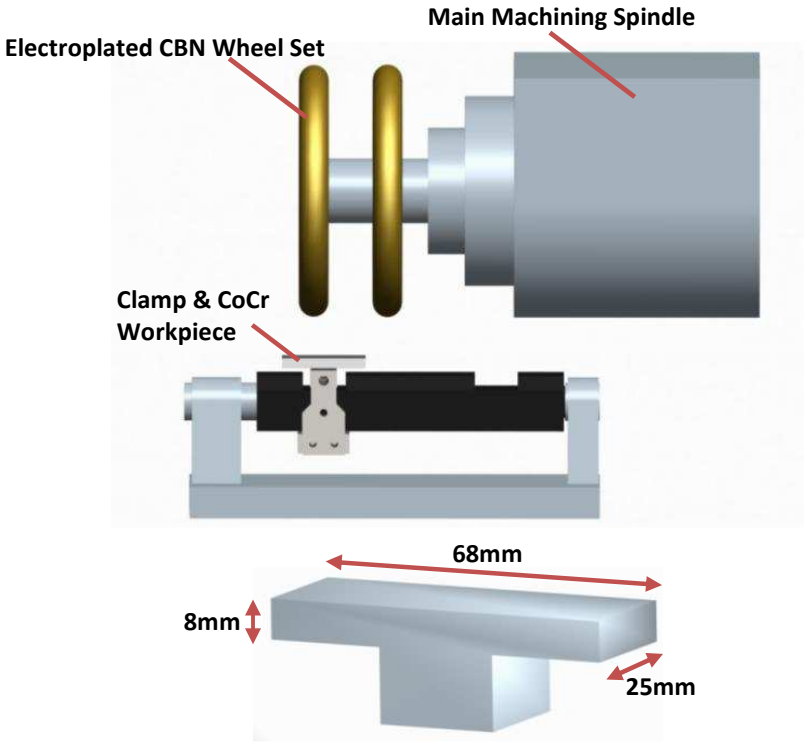

Fig. 1. (a) Machining Setup, (b) Workpiece

The total power of the spindle motor, as well as drive positions and total power of the feed drives were measured using Siemens Sinucom NC Trace software. The sample rate used was the maximum available at 333Hz, with a sampling interval of 3ms. An example of a digital drive power signal recorded from Sinucom Trace for the main spindle is shown in Fig. 2. The region denoted by A shows the power consumed as the wheel approaches the workpiece. The power here is the power necessary for spinning the wheel at the required speed with coolant turned on. Region B denotes the power consumed during machining of the workpiece. Region C is where the wheel has exited the workpiece.

Spindle active power recorded in this way was the total power including the power necessary for rotation of the spindle as well as the cutting power. Thus the cutting power was obtained by subtracting the rotary power components from the corresponding total. The power necessary for spindle rotation, as shown in Region A, was measured in all tests and was found to be rotational-speed dependent, varying between approximately 730 to 1400 Watts.

A Mitutoyo Suftest SJ-400 with a 5μm nominal stylus tip was used here to measure the surface roughness average parameter, Ra. The evaluation length was 2.5mm, the cut-off length λc 2.5mm, and the speed was 0.5mm/s. The average roughness parameter was measured 5 times along each tool path to obtain the mean value.

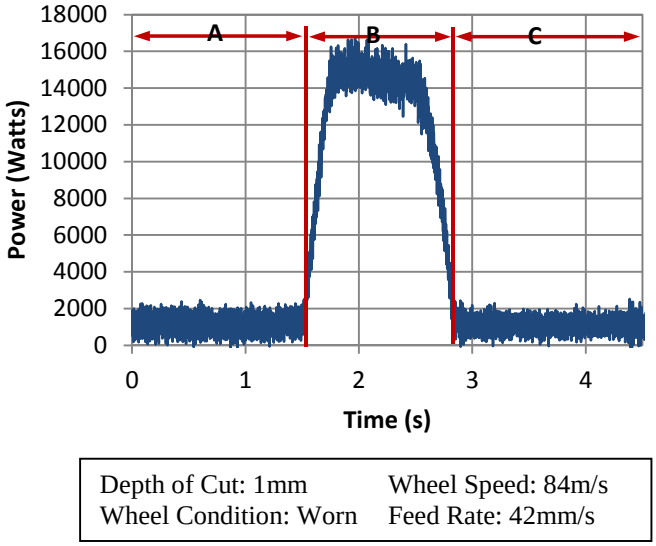

Fig. 2. Example of power trace of digital drive signal

Taguchi methods can be used for screening purposes, when the experimenter is interested in addressing main effects in an efficient manner with a minimum of experimental runs. These are fractional factorial experiments. The fractional factorial design focuses on main effects and lower-order interactions while assuming that higher order interactions between the variables do not exist. Such a design is suitable for a screening process, where many parameter settings have to be selected and it is necessary to keep the study size at a minimum number of runs [9]. In the case of a production process, often-times it is the one- or two-way interaction effects that are the main interest, rather than 4-way interactions between variables such as feed rate, rotational speed, depth of cut and tool condition.

This study utilized a modified L16 Taguchi fractional factorial orthogonal array with analysis of variance (ANOVA) to evaluate the effect of cutting conditions on power, specific energy and surface roughness. Each test was replicated 3 times. The factor levels were chosen based on previous experience with a reasonable spread in values, for feed rate, wheel speed and depth of cut. The test array and corresponding results are shown in Table 1.

When machining with electroplated CBN wheels, the wheels are not dressed therefore the wheel runs from sharp at the beginning of its life to dull and worn near the end of its life. It is not always known when exactly the appropriate time to change these wheels is, or indeed what the effect of machining with a worn tool is. Therefore a parameter of wheel condition was chosen to evaluate the effect of machining on spindle cutting power. A new wheel and a second wheel deemed to be near the end of its life were used in the investigation.

Optical micrographs of the worn wheel surface, as shown in Fig. 3, reveal wear on the CBN grains by attrition, grain fracture and grain pullout [10].

The areal packing density was measured using a 5MP usb polarized microscope camera, Dinolite AM7013MZT, at 20x magnification. The average of the areal packing density for 10 images of an area of 16mm^2 for both the new and worn wheel was taken.

Measurements are presented in Table 2. The areal packing density is calculated as 9.7 grains/mm^2 for the new wheel and 9.0grains/mm^2 for the worn wheel. The difference between the two values indicates that a small amount of grain pullout has taken place during the wheels life.

Table 1. Taguchi L16 Design Array

Test Number	Wheel Speed (m/s)	Feed Rate (mm/s)	Depth of Cut (mm)	Wheel Condition	Cutting Power (Watts)	Specific Energy (J/mm^3)	Surface Roughness Ra (μm)
1	52	42	0.5	New	2842	29.3	8.22
2	52	51	0.5	New	3227	27.7	8.15
3	52	59	1	Worn	12122	31.7	7.50
4	52	68	1	Worn	12599	28.8	7.63
5	63	42	0.5	Worn	7162	73.7	7.61
6	63	51	0.5	Worn	7187	61.7	7.54
7	63	59	1	New	7249	19.0	8.08
8	63	68	1	New	8545	19.6	8.18
9	73	42	1	New	7219	26.4	8.18
10	73	51	1	New	7399	22.6	8.13
11	73	59	0.5	Worn	8280	60.9	7.45
12	73	68	0.5	Worn	9831	63.2	7.60
13	84	42	1	Worn	13287	48.7	7.54
14	84	51	1	Worn	13667	41.7	7.64
15	84	59	0.5	New	3930	28.9	8.31
16	84	68	0.5	New	3694	23.8	8.05

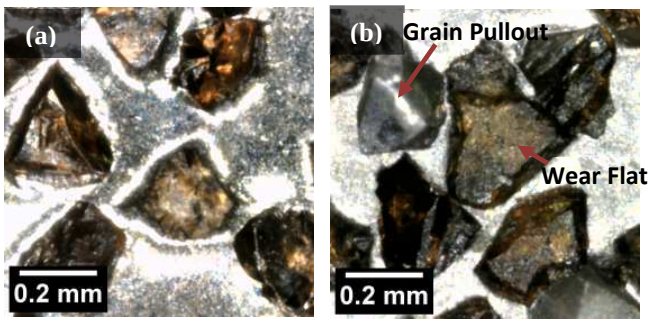

Fig. 3. Micrograph of wheel surface, (a) New wheel, (b) Worn wheel

After the tests were completed, replicas of the wheel surface were taken using Microset 101TH material at 5 random locations around the wheel surface of both wheels. Replicas of the wheel surface were taken in order to avoid cutting a section out of the steel hub which could be replated and reused. Optical micrographs of the replicas were taken with a Leica DMLM microscope fitted with a 5MP Canon Powershot S50 camera at 10x magnification. These micrographs of the replicas reveal flat reflective areas which represent the wear flats on the active grains, an example is shown in Fig. 4. Subsequently the wear flat

area, *A*, which is the percentage of the wheel surface consisting of wear flats, was estimated by calculating the wear flat by overlaying a fine grid on the optical micrographs [11].The average value for the wear flat area, *A*, was found to be 2.1% for the worn wheel. It is likely that any underestimation of wheel wear relates to replication inaccuracies.

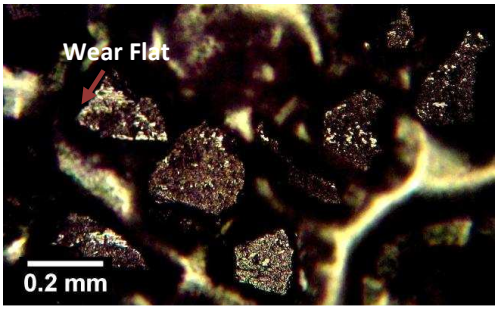

Fig. 4. Example of wear flats taken from replica on worn wheel

Surface topography measurements of the replicas were taken using an Omniscan MicroXam white light interferometer. Fig. 5 shows 3D topographic maps (curvature compensated) taken from replicas of both the new and worn B301 wheel. The parameters density of summits, Sds , and summit curvature, SSc, were calculated from the 3D white light data. The results are shown in Table 2. It is clear that there is a considerable difference between the new and worn wheels in terms of grain morphology, whereas the concentration of grains does not vary by a large amount.

Table 2. Wheel Condition Metrics

Wheel Condition	Areal Packing Density, Co (Grains/mm^2)	Sds (Peaks/mm^2)	SSc (mm^{-1})	Wear Flat Area (%)
New	9.7	66.2	56.2	
Worn	9.0	52.9	37.9	2.09

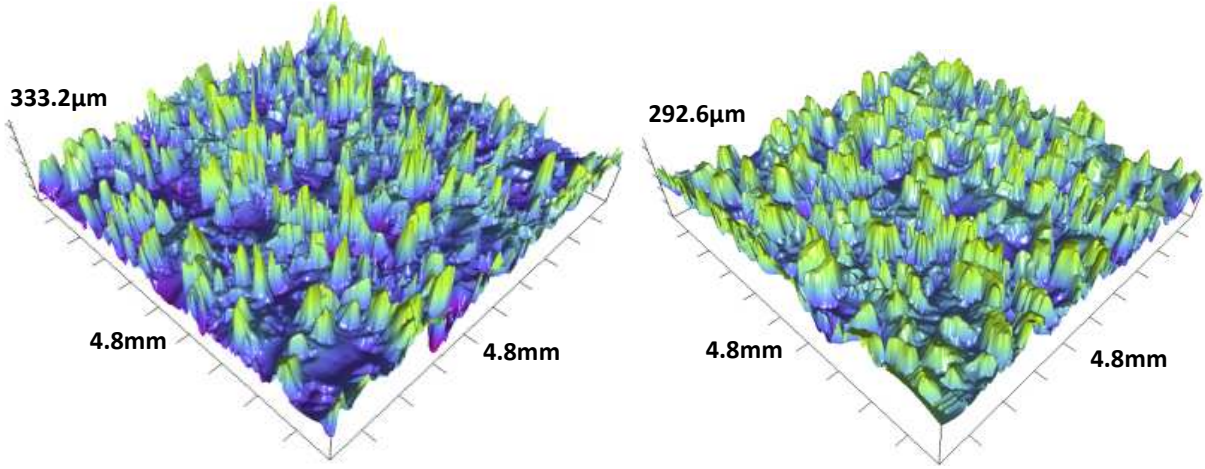

Fig. 5. 3D Topographic maps of (a) New B301 Wheel (b) Worn B301 Wheel

3. EXPERIMENTAL RESULTS & DISCUSSION

Figure 6 and Table 3 show the main effects plot and corresponding ANOVA results relating to means for cutting power for the duration of machining for the tests. In general, recorded cutting power for the various parameters varied between 3kW and 13kW. Analysis of variance identified that for the cutting power response, all of the main factors were statistically significant for the alpha value of 5%. Wheel condition had the highest percent contribution ratio (PCR) of 52.3% for cutting power.

This is as expected, as power and forces have been shown previously to increase significantly with wheel wear [8, 10]. Depth of cut has the second highest PCR of 42.1%. Wheel speed, and feed rate both have a significant effect on the cutting power response, however their PCR values were much lower, at 1.4% and 1.1% respectively. The error level with a PCR of 3.1% was also quite low.

These results show that spindle cutting power from the NC data is sensitive to changes in process parameters, and that power monitoring in this case is a reliable indicator of tool wear over a variety of machining parameters.

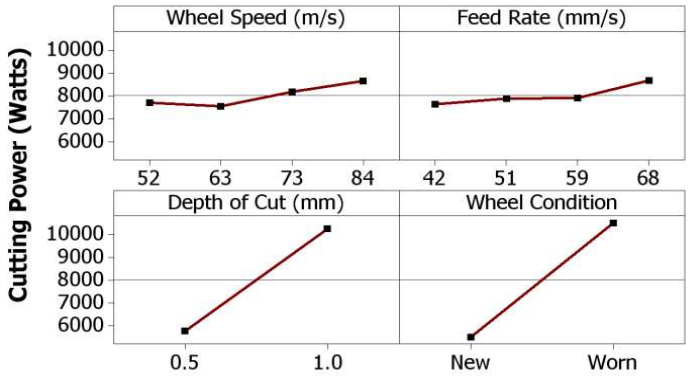

Fig. 6. Main Effect Plot for Cutting Power (Watts)

Table 3. ANOVA Results for Cutting Power

Source	DF	Seq SS	Exp SS	F	P	PCR (%)
Wheel Speed (m/s)	3	9054780	7932609	8.07	0.000	1.4
Feed Rate (mm/s)	3	7325870	6203699	6.53	0.001	1.1
Depth of Cut (mm)	1	242111238	241737181	647.26	0.000	42.1
Wheel Condition	1	300466576	300092519	803.26	0.000	52.3
Error	39	14588213				3.1
Total	47	573546677				

DF = Degrees of freedom
Seq SS = Sequential sums of squares
Exp SS = Expected sums of squares
F = F-test
P = Probability value
PCR = % contribution ratio

The specific energy, *u*, was calculated as follows:

$$u = \frac{P}{v_w A_s} \tag{1}$$

Where P is the cutting power, v_w, the feed rate and where A_s, the area of material removal due to the toric shaped wheel with a major and minor radius is;

$$A_s = R^2 cos^{-1}\left(\frac{R-a}{R}\right) - (R-a)\sqrt{2Ra - a^2} \tag{2}$$

Where R is the minor tool radius of 12mm in this case and a is the depth of cut. For a depth of cut of 0.5mm and 1mm the machined track width, w, was approximately 6.8mm and 9.6mm respectively.

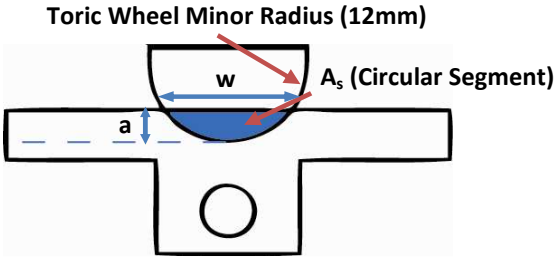

Fig. 7. Diagram of Wheel Intersecting with Workpiece

Main effect plots for means of specific energy are shown in Fig. 8. As with cutting power, analysis of variance identified all factors were significant at the 5% level.

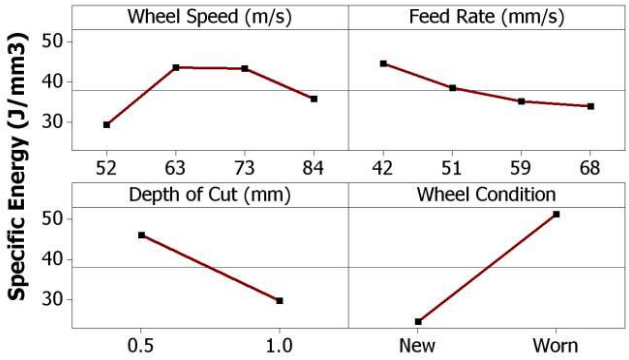

Fig. 8. Main effect plot for specific energy

The increase in mean specific energy with tool wear as shown in Fig. 8 to a value of over 50J/mm^3 is particularly significant here, with a PCR of 59%. This value is quite high, illustrating the extreme increase in energy entering the workpiece as the tool wears. The other contributing factor to increased specific energy in the process is the wheel speed and feed rate. With a relatively slow wheel speed and feed rate of 63m/s and 42mm/s

respectively, along with a depth of cut of 0.5mm and a worn wheel, the specific energy is shown rising to a maximum test value of 74J/mm^3. It is also interesting to note here that as the depth of cut increases from 0.5mm to 1mm the specific energy is shown to decrease. This becomes a significant issue in terms of efficiency in machining and reducing the effect of residual stress – with a larger depth of cut the energy is dispersed over a greater surface area and thus the specific energy is reduced.

Table 4. ANOVA Results for Specific Energy

Source	DF	Seq SS	Exp SS	F	P	PCR (%)
Wheel Speed (m/s)	3	1648.8	1622.2	62.09	0.000	11.2
Feed Rate (mm/s)	3	818.9	792.3	30.84	0.000	5.4
Depth of Cut (mm)	1	3198.7	3189.8	361.39	0.000	21.9
Wheel Condition	1	8530.0	8521.1	963.73	0.000	58.6
Error	39	345.2				2.9
Total	47	14541.6				

It has been noted previously that the temperatures generated during the grinding process are a direct consequence of the energy going into the process[11]. Consequently, specific energy has been used previously as a burn threshold method for avoiding thermal damage on the workpiece [12-14]. Ensuring temperatures in the process are as low as possible is also beneficial in terms of avoiding residual stresses. Residual tensile stresses, which can be responsible for deformation of the workpiece after machining, are caused mainly by thermally induced stresses and deformation associated with the temperatures during the process [15]. Thus lower specific energies are desirable when machining equally in terms of reducing the risk of thermal damage and of residual stresses.

Another point of interest is that an increase in feed rate results in a decrease in specific energy. This is in agreement with other publications for different metal alloys, where it was seen that higher material removal rates resulted in lower specific energy [12],[16]. The volumetric removal rates studied here ranged from 97mm^3/s to 473mm^3/s. The results here indicate the most optimal conditions for low specific energy would be to run the process with increased volumetric removal rates in order to avoid high specific energies during machining. This may be particularly beneficial when tool wear starts to become a significant factor as the wheel approaches the end of its useful life.

Further work needs to be undertaken in order to determine the optimal volumetric removal rate with respect to specific energy and temperature. Maximum permissible forces in the machining clamp and spindle may also be an issue when considering and increase volumetric removal rates.

Figure 9 shows the main effect plots for means of surface roughness, Ra value. The Ra values quoted are quite high, ranging from 7.5μm and 8.1μm. This is due to the geometric influence of the curved profile of the machined track. As expected, the workpiece surface roughness was shown to decrease with wheel wear, with a correspondingly high PCR of 79% [10]. It can be seen that there is a considerable difference in the Ra value between the new and worn wheels of ~0.6μm.

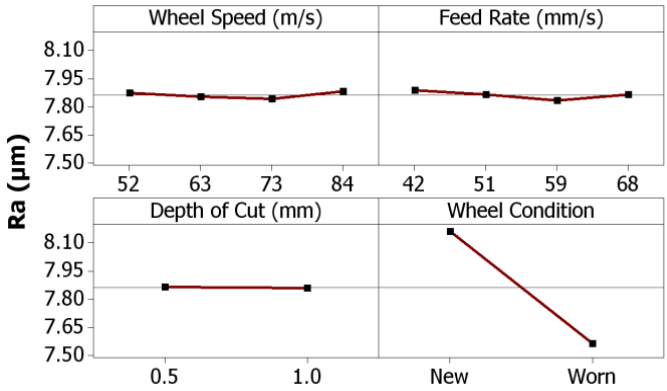

Fig. 9. Main Effect plot for Surface Roughness

Table 5. ANOVA Results for Surface Roughness

Source	DF	Seq SS	Exp SS	F	P	PCR (%)
Wheel Speed (m/s)	3	0.01277	-0.06982	0.15	0.926	0.0
Feed Rate (mm/s)	3	0.01679	-0.0658	0.20	0.894	0.0
Depth of Cut (mm)	1	0.00035	-0.02718	0.01	0.911	0.0
Wheel Condition	1	4.30441	4.27688	156.36	0.000	79.1
Error	39	1.07364				20.9
Total	47	5.40797				

The level of error for the surface roughness is quite high with a PCR of 21%, this is likely due to the highly variable surface produced by grinding with a relatively large mean grain diameter of 301µm. The results for wheel speed, feed rate and depth of cut show little change in the surface roughness value between parameters. Therefore an increase in the material removal rate during machining could be achieved with minimal effect on surface roughness, which in turn could be beneficial in terms of avoiding high energy and temperatures.

4. CONCLUSION

This paper investigates the power monitoring of an abrasive machining operation using an NCK machine data monitoring method. There is a distinct advantage for industrial users in the implementation and development of this method as it eliminates the need for installation of external sensors such as power cells, and the added investment cost that goes with it.

Spindle cutting power has been shown to be sensitive to changes in wheel speed, feed rate, depth of cut and wheel condition. In the case of wheel condition a difference in spindle cutting power between a new and worn wheel was shown to be in the range of 4kW and for

specific energy, u, in the range of 25J/mm^3. This significant result implies that spindle power monitoring with an NCK based application may be suitable for tool wear detection in the case of machining with superabrasives and difficult to machine alloys.

It has also been shown it is possible to achieve a reduction in specific energy through an increase in feed rate while maintaining reasonable workpiece surface roughness.

ACKNOWLEDGEMENTS

The authors would like to acknowledge that this research has been carried out as part of a project funded by the Irish Research Council for Science, Engineering and Technology (IRCSET) and DePuy Ireland, Johnson and Johnson with additional finance provided by the Department of Mechanical Engineering, Trinity College Dublin. The authors would also like to thank Mr. John Quin and Mr. Ruairi Cullinane, DePuy Ireland, for their support in carrying out machining tests, as well as Prof. Andrew Torrance for advice on wear measurement.

REFERENCES

[1] TETI R., JEMIELNIAK K., O'DONNELL G., and DORNFELD D., 2010, *Advanced monitoring of machining operations*, CIRP Annals - Manufacturing Technology, 59/717-739.

[2] PRITSCHOW G., ALTINTAS Y., JOVANE F., KOREN Y., MITSUISHI M., TAKATA S., Van BRUSSEL H., WECK M., and YAMAZAKI K., 2001, *Open Controller Architecture - Past, Present and Future*, CIRP Annals - Manufacturing Technology, 50/463-470.

[3] BRECHER C., QUINTANA G., RUDOLF T., and CIURANA J., 2010, *Use of NC kernel data for surface roughness monitoring in milling operations*, The International Journal of Advanced Manufacturing Technology, 1-10.

[4] QUINTANA G., RUDOLF T., CIURANA J., and BRECHER C., 2011, *Using kernel data in machine tools for the* indirect *evaluation of surface roughness in vertical milling operations*, Robotics and Computer-Integrated Manufacturing, 27/1011-1018.

[5] QUINTANA G., RUDOLF T., CIURANA J., and BRECHER C., 2011, *Surface roughness prediction through internal kernel information and external accelerometers using artificial neural networks*," Journal of Mechanical Science and Technology, 25/2877-2886.

[6] NIINOMI M., 2010, *Metals for biomedical devices*, ed: Woodhead Publishing, Oxford.

[7] DENKENA B., de LEON L., TURGER A., and BEHRENS L., 2010, *Prediction of contact conditions and theoretical roughness in manufacturing of complex implants by toric grinding tools*, International Journal of Machine Tools and Manufacture, 50/630-636.

[8] GUO C., SHI Z., ATTIA H., and MCINTOSH D., 2007, *Power and Wheel Wear for Grinding Nickel Alloy with Plated CBN Wheels*, *CIRP Annals - Manufacturing Technology*, 56/343-346.

[9] ROSS P. J., 1996, *Taguchi Techniques for Quality Engineering*: McGraw-Hill, New York

[10] SHI Z. and MALKIN S., 2006, *Wear of electroplated CBN grinding wheels*, Journal of manufacturing science and engineering, 128/110.

[11] MALKIN S. and GUO C., 2008, *Grinding technology: theory and applications of machining with abrasives*, second ed. New York: Industrial Pr.

[12] STEPHENSON D. J., JIN T., and CORBETT J., 2002, *High Efficiency Deep Grinding of a Low Alloy Steel with Plated CBN Wheels*, *CIRP Annals - Manufacturing Technology*, 51/241-244.

[13] ROWE W. B., PETTIT J. A., BOYLE A., and MORUZZI J. L., 1988. *Avoidance of Thermal Damage in Grinding and Prediction of the Damage Threshold*, CIRP Annals - Manufacturing Technology, 37/327-330.

[14] BELL A., JIN T., and STEPHENSON D. J., 2011, *Burn threshold prediction for High Efficiency Deep Grinding*, *International Journal of Machine Tools and Manufacture*, 51/433-438.

[15] MALKIN S. and GUO C., 2007, *Thermal Analysis of Grinding*, CIRP Annals - Manufacturing Technology, 56/760-782.

[16] HOOD R., LECHNER F., ASPINWALL D., and VOICE W., 2007, *Creep feed grinding of gamma titanium aluminide and burn resistant titanium alloys using SiC abrasive*, International Journal of Machine Tools and *Manufacture*, 47/1486-1492.